DETECTING THE LAVA FLOW DEPOSITS FROM 2018 ANAK KRAKATAU ERUPTION USING DATA FUSION LANDSAT-8 OPTIC AND SENTINEL-1 SAR

Suwarsono[1]*, Indah Prasasti[1], Jalu Tejo Nugroho[1], Jansen Sitorus[1], and Djoko Triyono[2]
[1]Remote Sensing Application Center,
Indonesian National Institute of Aeronautics and Space (LAPAN)
[2]Department of Physics, Faculty of Mathematic and Natural Sciences,
Universitas Indonesia
*E-mail: suwarsono@lapan.go.id
Received: 4 December 2018; Revised: 24 December 2018; Approved: 27 December 2018

Abstract. The increasing volcanic activity of Anak Krakatau volcano has raised concerns about a major disaster in the area around the Sunda Strait. The objective of the research is to fuse Landsat-8 OLI (Operational Land Imager) and Sentinel-1 TOPS (Terrain Observation with Progressive Scans), an integration of SAR and optic remote sensing data, in observing the lava flow deposits resulted from Anak Krakatau eruption during the middle 2018 eruption. RGBI and the Brovey transformation were conducted to merge (fuse) the optical and SAR data. The results showed that optical and SAR data fusion sharpened the appearance of volcano morphology and lava flow deposits. The regions are often constrained by cloud cover and volcanic ash, which occurs at the time of the volcanic eruption. The RGBI-VV and Brovey RGB-VV methods provide better display quality results in revealing the morphology of volcanic cone and lava deposits. The entire slopes of Anak Krakatau Volcano, with a radius of about 1 km from the crater is an area prone to incandescent lava and pyroclastic falls. The direction of the lava flow has the potential to spread in all directions. The fusion method of optical Landsat-8 and Sentinel-1 SAR data can be used continuously in monitoring the activity of Anak Krakatau volcano and other volcanoes in Indonesia both in cloudy and clear weather conditions.

Keywords: *lava flow, Anak Krakatau, data fusion, Landsat-8, Sentinel-1 SAR*

1 INTRODUCTION

Anak Krakatau Volcano, which is located on The Sunda Strait, administratively located in the South Lampung Regency, is one of the 129 Indonesian active volcanoes. Anak Krakatau volcano itself, since its emergence in 1929 until now, has erupted at least 80 times. In other words, the eruption of which has occurred every year in the form of explosive or effusive eruptions. The time of the volcano is between 1 - 8 years but the eruption can occur 1 - 6 times a year (Sutawidjaja 2006).

The eruption of Krakatau on 27 August 1883, was one of the most powerful eruptions in history. The eruption destroyed most of the volcanic island of Krakatoa in the strait separating the land of Sumatra and Java. Then, there was an eruption from 1927 to 1929 and produced a new volcano known as Anak Krakatau. Until now, this volcano continues to experience growth (Agustan *et al.* 2012).

The eruption from October 2007 till August 2008 was characterized by Strombolian activity. During this eruption, a new crater was formed on

http://dx.doi.org/10.30536/j.ijreses.2018.v15.a3078

the southwestern flank of the volcano just below the main crater, producing ash plumes as well as lava flows. (Agustan *et al.* 2012).

Based on the records from the Center for Volcanology and Geological Disaster Mitigation (http://www.vsi.esdm.go.id /index.php /gunungapi/aktivitas-gunungapi), the last eruption in 2018 to date occurred on June 25-26, July 16, August 3, August 17, August 23, October 3 and 6, and November 16 and 26. The eruption on July 23, 2018 and September 23, in addition to removing volcanic ash, produced incandescent lava melt, down the slope, leads South and South East to reach the sea.

Many studies on this volcano mainly discuss about the famous Krakatau eruption on 1883 and how it caused tsunamis (Rampino and Self 1982; Francis 1985; Dörries 2003); the growth of Anak Krakatau and Anak Krakatau (Sutawidjaja 1997, 2006; Deplus *et al.* 1995; Ibs-von Seht 2008), and the ground deformation of Anak Krakatau (Agustan *et al.* 2012). However, the studies on distribution of lava flow from recent eruption are still limited.

The objective of the research is to observe the lava flow deposits resulted from Anak Krakatau eruption during middle 2018 eruption. The fusion of Landsat-8 OLI (Operational Land Imager) and Sentinel-1 TOPS (Terrain Observation with Progressive Scans), as the integration of SAR and optic remote sensing data, was used to identify of the lava flow deposits.

Landsat-8 satellite, the newest satellite of Landsat satellite series, is operated by the National Aeronautics and Space Administration (NASA) and the Department of the Interior United States of Geological Survey (USGS). Landsat-8 has the advantages to its predecessors.

Tabel 1-1: OLI spectral and spatial specification (Iron *et al.*, 2012)

Bands	Band with (μm)	GSD (m)
1	0.433 – 0.453	30
2	0.450 – 0.515	30
3	0.525 – 0.600	30
4	0.630 – 0.680	30
5	0.845 – 0.885	30
6	1.560 – 1.660	30
7	2.100 – 2.300	30
8	0.500 – 0.680	15
9	1.360 – 1.390	30

Table 1-2: TIRS spectral bands and spatial resolution (Irons *et al.* 2012)

Bands	Center wavelength (μm)	Minimum lower band edge (μm)
10	10.9	10.6
11	12.0	11.5

Landsat-8 carries an Operational Land Imager (OLI), consists of nine spectral channels with a spatial resolution of 30 m (15 m for the panchromatic channel), and the Thermal Infrared Sensor (TIRS) which will measure land surface temperature in two thermal bands with a 100 m spatial resolution (Irons *et al.* 2012) (Table 1-1 and Table 1-2).

The Sentinel-1 is a C-band (5.36 GHz) SAR data product of European Space Agency (ESA). The product has been acquired in four different modes namely Stripmap (SM), Interferometric Wide swath (IW), Extra-Wide swath (EW) and Wave (WV). The instrument was designed with one transmitter and two receiver chain. It supports operation in a single and dual polarization (Periasamy 2018). The data has been acquired with Ground Swath width of 250 km and Azimuth pixel spasing of 14.1 m. The satellite has Orbital Repeat Cycle of 12 days (Martinez *et al.* 2016).

In many applications, the quality of remote sensing image data is a very important aspect. In many situations, the data from one type of sensor is not enough to provide an accurate analysis of observed objects. The basic purpose of data fusion is to get more quality information compared to what we will get from a single sensor. Therefore, the fusion of multi-sensor data has been an intense field of research in recent years (Reulke *et al.* 2013). Optical and radar images have two different aspects of analyzing satellite imagery. Optical images such Landsat-8 OLI have the advantages in terms of providing more semantic information obtained from multispectral data. The disadvantage is that the presence of clouds will be a barrier to analyzing objects under the cover. Meanwhile, radar images, such as Sentinel-1 SAR, have the advantages in terms of not being affected by clouds or recording time (day or night). By combining both types of data, it is expected to improve image quality for the analysis of objects to be observed.

So, by combining the two types of data (Landsat-8 and Sentinel-1 SAR), it is expected that images with better quality will be obtained for the interpretation of lava flow deposits.

2 MATERIALS AND METHODOLOGY

2.1 LOCATION AND DATA

The research location is Krakatau volcano complex. The Krakatau complex consists of four islands which are Sertung, Panjang, Rakata, and Anak Krakatau. Sertung, Panjang, and Rakata Island are the remnants of the caldera collapse due to the 1883 Krakatau eruption. Anak Krakatau emerged in 1929, was about 46 years after the paroxysmal eruption. This volcano is a stratovolcano and was built by alternating layers of lava and pyroclastic deposits that had been erupted since the 1930s. Since its emergence at sea level in 1929 until now, the growth of Anak Krakatau Volcano is very fast. The height of the Anak Krakatau volcano peak from 1930 to 2005, for 75 years, reached 315 m. The estimated acceleration of growth is an average of four meters per year (Sutawidjaja 1997; 2006).

The Krakatau complex is covered by Landsat-8 satellite coverage for path/row 123/064. Administratively, the research sites are included in the areas of the Lampung Selatan Regency, Lampung Province. Figure 2-1 shows the location of the research.

Figure 2-1: Location of the study Anak Krakatau Volcano (red rectangle), coverage of Landsat-8 for path/row 123/064 (green rectangle). Map source: http://landsat-catalog.lapan.go.id/.

The optical data used were Landsat-8, path / row 123/064. The time of data acquisition was 1 October 2018. Landsat-8 data were obtained from The Remote Sensing Technology and Data Center of Indonesian National Institute of Aeronautics and Space (LAPAN), through the http://landsat-catalog.lapan.go.id/. The data format is GeoTIFF. The level of Landsat-8 is level one terrain-corrected product (L1T). The data that available to users is the radiometrically and geometrically corrected image (Zanter 2015). The L1 Single Look Complex (SLC) products of Sentinel-1 TOPS were obtained from Alaska Satellite Facility through https://www.asf.alaska.edu/. The Sentinel-1 TOPS IW mode is the main mode of operations for the systematic monitoring of large land and coastal areas (Torres *et al.* 2012).

Table 2-1: Sentinel 1 Interferometric wide Swath Mode SLC Product Parameters (Martinez *et al.* 2016).

Mode id.	IW1	IW2	IW3
Incidence angles	32.9°	38.3°	43.1°
Slant range resolution	2.7 m	3.1 m	3.5 m
Range Bandwidth	56.5 MHz	48.3 MHz	42.79 MHz
Azimuth resolution	22.5 m	22.7 m	22.6 m
Processing Bandwidth	327 Hz	313 Hz	314 Hz
Doppler Centroid span (Δf_{DC})	5.2 kHz	4.4 kHz	4.6 kHz
Slant range pixel spacing		2.3 m	
Range sampling frequency		64.35 MHz	
Azimuth pixel spacing		14.1 m	
Azimuth sampling frequency		486.49 Hz	
Azimuth steering angle		± 0.6°	
Burst length ($T_{focused}$)		2.75s / ≈ 20 km	
Ground Swath width		250 km	
Slice length		170 km	
Orbital Repeat Cycle		12 days	
Orbit height		698 – 726 km	
Wavelength		5.547 cm	
Polarization		Single (HH or VV) or Dual (HH+HV or VV+VH)	

Table 2-1 show the Sentinel 1 Interferometric Wide Swath Mode, SLC product parameters. The SAR data used were Sentinel-1 TOPS, beam mode Interferometric Wide swath (IW), Single Look Complex (SLC) products, flight direction Descending, polarization VV and VH, path/frame 47/614. The acquisition of the data was on 17 September 2018. The acquisition date is selected as it is close to Landsat-8 data acquisition time.

2.2 METHODS

2.2.1 DATA CALLIBRATION

Landsat-8 OLI data were converted to Top of Atmosphere (TOA) spectral radiance. Then, OLI data were converted to TOA reflectance. The following equation is used to convert DN values to TOA reflectance for OLI data as follows (Zanter 2015):

$$\rho\lambda' = M_\rho Q_{cal} + A_\rho \qquad (2\text{-}1)$$

in which $\rho\lambda'$ is TOA planetary reflectance (without correction for solar angle). M_ρ is Band-specific multiplicative rescaling factor, A_ρ is band-specific additive rescaling factor, and Q_{cal} is quantized and calibrated standard product pixel values (DN). Sun angle correction of TOA reflectance can be calculated by using the following equation (Zanter 2015):

$$\rho\lambda = \frac{\rho\lambda'}{\cos(\theta sz)} = \frac{\rho\lambda'}{\sin(\theta se)} \qquad (2\text{-}2)$$

in which $\rho\lambda$ is TOA planetary reflectance, θ_{SE} is local sun elevation angle. θ_{SZ} is local solar zenith angle, $\theta_{SZ} = 90° - \theta_{SE}$.

TOA reflectance does not correct the atmospheric effects. Thus DOS1 (Dark Object Subtraction 1) was implemented for converting Landsat images from TOA reflectance to surface reflectance (Chavez 1996). The DOS1 method is very simple because it doesn't require any information about atmospheric conditions, but the results are not as accurate as the Landsat Surface Reflectance High Level Data

Products. DOS1 method was conducted for atmospheric correction.

Sentinel-1 TOPS IW consists of VH and VV polarization. The Level-1 GRD (Grid) product was derived from internal Side Looking Complex (SLC). The Radiometric Calibration was performed for Amplitude imageries of VV and VH using calibration parameter A_σ to transform the radar backscattering into Radar Cross Section (σ°) (Equation 2-3) (Periasamy 2018).

$$\sigma° = DN^2 / A\sigma^2 \qquad (2\text{-}3)$$

in which DN represents Digital Number in the SAR Imagery. The results of the procedure (Eq. 2-3) are in $\sigma_{VV}°$ and $\sigma_{VH}°$ which are the conversion products from slant range to ground range.

The speckle reduction was performed by using Refined Lee filter to remove the noise and to smoothen the imagery. Then the Range Doppler Correction is performed to the speckle removed imagery to position the data geographically. Sigma naught (σ°) is the radar reflectivity per unit area in ground range. Sigma naught related to power returned to the antenna from the ground. Sigma naught values are directly related to the ground. The SRTM90 DEM produced from the U.S. Geological Survey (USGS) was used in this calibration processes.

2.2.2 DATA FUSION OF OPTICAL AND SAR POLARIMETRIC

To observe the eruption activities, volcano morphology, and lava flow deposits resulted from the eruption, both Landsat-8 optical and Sentinel-1 TOPS SAR were used. RGBI transformation was conducted to merge (fuse) the optical and SAR data. RGBI transformation is a simple method for data fusion. In this step, for RGBI transformation, band $SWIR_s$ (band 6), NIR (band 5), and RED (band 4) of Landsat-8 were input as Red, Green and Blue channel respectively. The combination band 6, 5 and 4 of Landsat-8 is useful for lava deposits identification. From the band combination, the lava deposit object looks reddish, the vegetation looks greenish and the water appears black or bluish. Then the sigma naught backscatter $\sigma_{VV}°$ and $\sigma_{VH}°$ of Sentinel-1 TOPS were input as intensity channel.

The Brovey transformation was also conducted for data fusion. The Brovey transformation can be used to merge images with different spatial and spectral characteristics (Jensen 2005). This transformation changes the reflectance value for each multispectral channel (R, G, and B), into new values (RP, GP, and BP). P is the co-registered band of higher spatial resolution images. The equation of Brovey Transformation used is as follows:

$$RP = R*P/R+G+B \qquad (2\text{-}4)$$

$$GP = G*P/R+G+B \qquad (2\text{-}5)$$

$$BP = B*P/R+G+B \qquad (2\text{-}6)$$

In this step, for Brovey transformation, band 6, 5, and 4 of Landsat-8 were input as Red, Green and Blue channel respectively. Then the sigma naught backscatter $\sigma_{VV}°$ and $\sigma_{VH}°$ of Sentinel-1 TOPS were input as P.

The images fusion of Landsat-8 optic and Sentinel-1 SAR, both from RGBI and Brovey were compared with the images fusion of Landsat-8, band 6,5,4 and panchromatic band (band 8), with the same methods.

3 RESULTS AND DISCUSSION

Optical and SAR data fusion are able to sharpen the appearance of volcano morphology and lava flow deposits. Especially in the region, it is often constrained by cloud cover and volcanic ash, which occurs when the volcanic eruption.

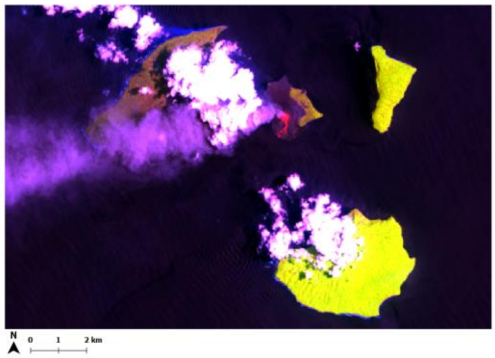

Figure 3-1: The eruption of Anak Krakatau Volcano, was captured and showed visually from Landsat-8 on 1 October 2018, composite false color RGB 654 (without pansharpen).

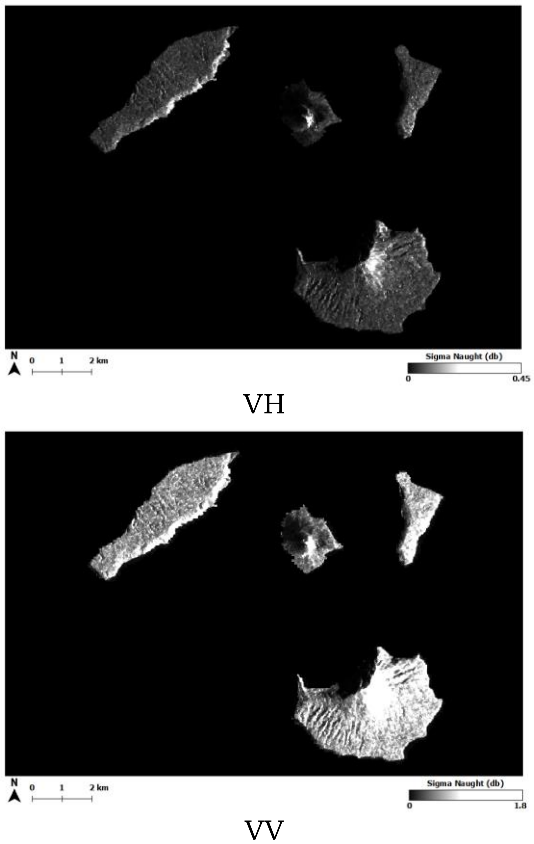

Figure 3-2: The sigma naught backscatter images derived Sentinel-1 TOPS acquisition date 17 September 2018 with VH and VV polarization.

The data fusion of Landsat-8 optical and Sentinel-1 TOPS SAR were used to observe the eruption activities and lava flow deposits resulted from the eruption. The morphology of Krakatau Complex, volcanic ash, pyroclastics, and lava flow deposits were analyzed based on the fusion images.

The eruption of Anak Krakatau Volcano, was captured and showed visually from Landsat-8 on 1 October 2018, composite false color RGB 654 (without pansharpen) (Fig. 3-1). Fig 3-2 showed the sigma naught backscatter images derived Sentinel-1 TOPS acquisition date 17 September 2018 with VH and VV polarization.

The fusion of Landsat-8 and Sentinel-1 are four fusion data sets, each of which is RGB-Intensity and RGB Brovey transformation for sigma naught backscatter VV ($\sigma_{VV}°$) and VH ($\sigma_{VH}°$). Figure 3-3 shows the results of the fusion of Landsat-8 and Sentinel-1 data on the Krakatau complex, just when the eruption occurred on October 1, 2018. Then, the Landsat-8 and Sentinel-1A fusion were compared with the images fusion of Landsat-8, band 6,5,4 and panchromatic band (band 8), with the same methods.

Based on the results of data fusion (Fig 3-3), it can be seen that the fusion of Landsat-8 and Sentinel-1 data using the RGBI-VV and Brovey RGB-VV methods provide the best results in accentuating lava deposits. These results have met the rules and objectives of data fusion, that are obtaining information of greater quality (Wald 1999), to form a unified picture (Khaleghi *et al.* 2013), and provide more reliable and accurate information (Luo *et al.* 2002).

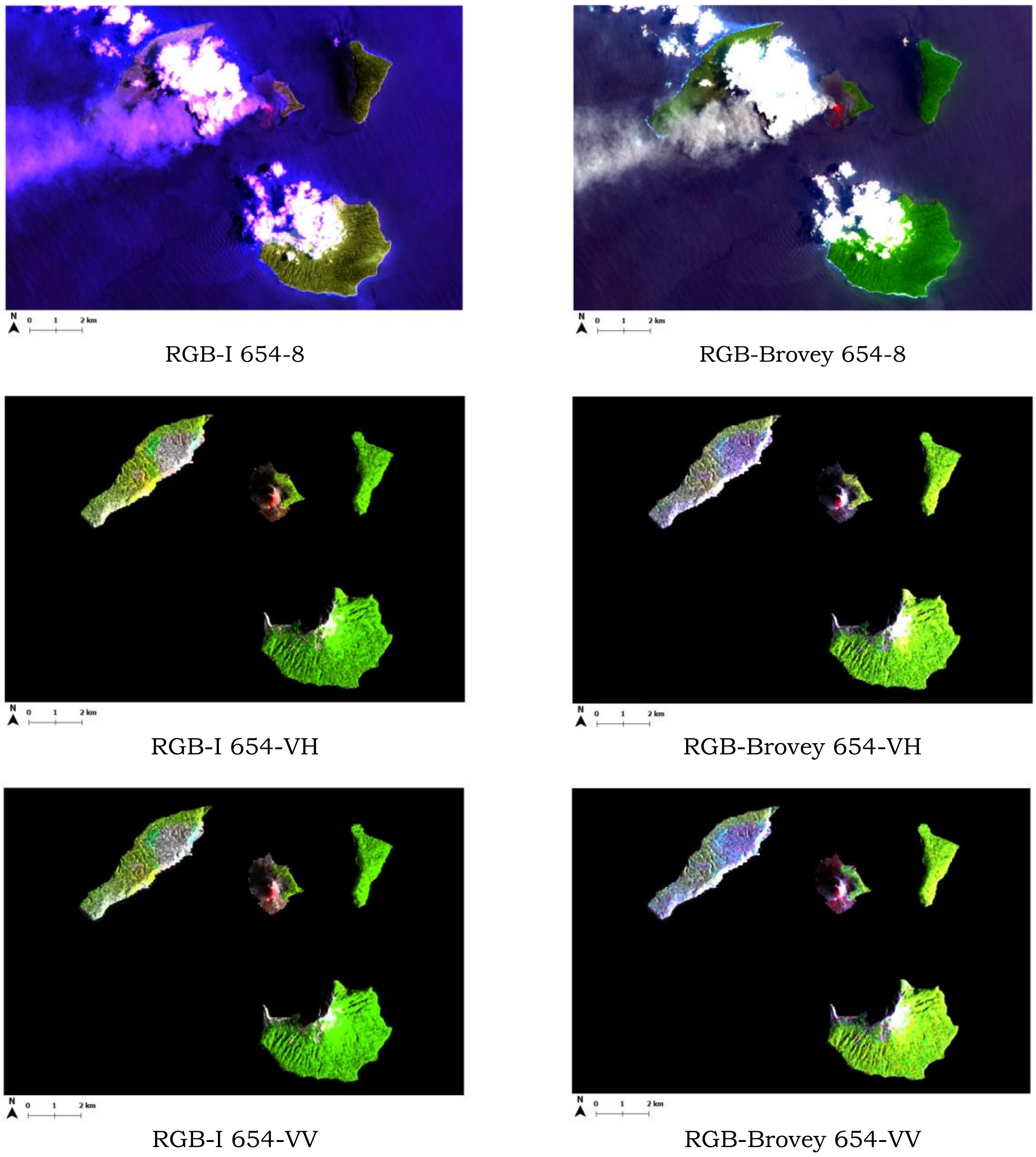

Figure 3-3: The results of fusion of Landsat-8 and Sentinel-1 data on the Krakatau complex with several methods. Red colors indicate the object of lava deposits.

Based on visual interpretation, it can be seen the presence of incandescent lava (appearing red), which flows down the southern slope. Previous lava deposits, appear to be dark brown, which predominantly spread towards the North, West and South slopes. The small portion of lava deposits are also exist on eastern slope. Based on observations of these images, it can be seen that the entire slopes of Anak Krakatau Volcano, with a radius of about 1 km from the crater, is an area prone to incandescent lava and pyroclastic falls. The direction of the lava flow has the potential to spread in all directions.

4 CONCLUSION

Optical Landsat-8 and Sentinel-1 SAR data fusion are able to sharpen the appearance of volcano morphology and lava flow deposits. Especially in the region, it is often constrained by cloud cover and volcanic ash, which occurs when the volcanic eruption. The RGBI-VV and Brovey RGB-VV methods provide better display quality results in revealing the morphology of volcanic cone and lava deposits. The entire slopes of Anak Krakatau Volcano, with a radius of about 1 km from the crater, is an area prone to incandescent lava and pyroclastic falls. The direction of the lava flow has the potential to spread in all directions. It is hoped that the fusion of optical Landsat-8 and Sentinel-1 SAR data can be used continuously in monitoring the activity of Anak Krakatau volcano and other volcanoes in Indonesia both in cloudy and clear weather conditions.

ACKNOWLEDGEMENTS

This paper is a part of the research activities entitled 'Development of Optical, SAR, LiDAR and / or GPS Data Fusion'. This research was funded by the Program of National Innovation System Research Incentive (INSINAS) in 2018, Ministry of Research Technology and the Higher Education Republic of Indonesia. Thank Mr. Suhermanto as the Group Leader in this activity and Dr. Mahdi Kartasasmita. Thank for the collegas from Remote Sensing Application Center of LAPAN, Remote Sensing Technology dan Data Center of LAPAN and Faculty of Mathematics and Natural Sciences who have provided suggestions for the discussion and suggestion. Thank also Dr. Hanik Humaida, Mr. Gede Suantika and Mr. Windi Cahya from Center for Volcanology and Geological Disaster Mitigation for discussion, collaboration, field surveys, and sharing information to support this research.

Sentinel-1 TOPS was provided by Alaska Satellite Facility. Landsat 8 OLI was provided by Remote Sensing Technology and Data Center, LAPAN. SRTM90 DEM was provided by the U.S. Geological Survey (USGS).

REFERENCES

Agustan, Kimata F., Pamitro YE, *et al.*, (2012), Understanding the 2007–2008 eruption of Anak Krakatau Volcano by combining remote sensing technique and seismic data. International Journal of Applied Earth Observation and Geoinformation 14:73-82.

Chavez Jr. PR, (1996), Image-based atmospheric corrections - revisited and improved. Photogrammetric Engineering & Remote Sensing 62(9):1025-1036.

Deplus C., Bonvalot S., Dahrin D., *et al*, (1995), Inner structure of the Krakatau volcanic complex (Indonesia) from gravity and bathymetry data. Journal of Volcanology and Geothermal Research 64(1–2):23–52.

Dörries M., (2003), Global science: the eruption of Krakatau. Endeavour 27(3), 113–116.

Francis PW, (1985), The origin of the 1883 Krakatau tsunamis. Journal of Volcanology and Geothermal Research 25(3–4): 349–363.

Ibs-von Seht M., (2008), Detection and identification of seismic signals recorded at Krakatau volcano (Indonesia) using artificial neural networks. Journal of Volcanology and Geothermal Research 176(4): 448–456.

Irons JR, Dwyer JL, and Barsi JA, (2012), The next Landsat satellite: The Landsat Data Continuity Mission. Remote Sensing of Environment 122:11-21.

Jensen JR, (2005), Introductory digital image processing, a remote sensing perspective. Pearson Prentice Hall. New Jersey.

Khaleghi B., Khamis A., Karray FO, *et al.*, (2013), Multisensor data fusion: A review of the state-of-the-art. Inform. Fusion (14)1:28–44.

Luo RC, Yih CC, and Lan Su K., (2002), Multisensor fusion and integration: Approaches, applications, and future research directions. IEEE Sensors J. 2(2):107–119.

Martinez NY, Iraola PP, Gonzales FR, *et al.*, (2016), Interferometric processing of Sentinel-1 TOPS Data. IEEE

Transactions on Geoscience and Remote Sensing 54(4):2220-2233.

Periasamy S., (2018), Significance of dual polarimetric synthetic aperture radar in biomass retrieval: An attempt on Sentinel-1. Remote Sensing of Environment 217: 537-549.

Rampino MR, and Self S., (1982), Historic eruptions of Tambora (1815), Krakatau (1883), and Agung (1963), their stratospheric aerosols, and climatic impact. Quaternary Research 18 (2): 127–143.

Reulke R., Giaquinto,G., Giovenco *et al.*, (2013), Optics and radar image fusion based on image quality assessment. 2013 Seventh International Conference on Sensing Technology, IEEE: 690-696.

Sutawidjaja IS, (1997), The activities of Anak Krakatau volcano during the years of 1992–1996. Annuals of the Disaster Prevention Research Institute 40: 13–22.

Sutawidjaja IS, (2006), Pertumbuhan Gunung Api Anak Krakatau setelah letusan katastrofis 1883. Jurnal Geologi Indonesia 1(3): 143-153.

Torres R., Snoeij P., Geudtner D., *et al.*, (2012), GMES Sentinel-1 mission, Remote Sensing of Environment 120: 9–24.

Wald L., (1999), Some terms of reference in data fusion. IEEE Transactions on Geoscience and Remote Sensing 37(3): 1190–1193.

Zanter K. (Ed)., (2015), Landsat 8 (L8) data users handbook, Version 1. Sioux Falls, South Dakota: Department of the Interior, U.S. Geological Survey.